Hyperspectral imaging for differentiation of foreign materials from pinto beans

Mehrubeoglu, Mehrube, Zemlan, Michael, Henry, Sam

Mehrube Mehrubeoglu, Michael Zemlan, Sam Henry, "Hyperspectral imaging for differentiation of foreign materials from pinto beans," Proc. SPIE 9611, Imaging Spectrometry XX, 96110A (1 September 2015); doi: 10.1117/12.2207797

Event: SPIE Optical Engineering + Applications, 2015, San Diego, California, United States

Hyperspectral imaging for differentiation of foreign materials from pinto beans

Mehrube Mehrubeoglu*[a], Michael Zemlan[b], Sam Henry[b]
[a]Hyperspectral Optical Property Instrumentation (HOPI) Laboratory, School of Engineering and Computing Sciences, Texas A&M University-Corpus Christi, 6300 Ocean Dr., Corpus Christi, TX, USA, 78412-5797; [b]Surface Optics Corp., 11555 Rancho Bernardo Rd., San Diego, CA, USA 92127

ABSTRACT

Food safety and quality in packaged products are paramount in the food processing industry. To ensure that packaged products are free of foreign materials, such as debris and pests, unwanted materials mixed with the targeted products must be detected before packaging. A portable hyperspectral imaging system in the visible-to-NIR range has been used to acquire hyperspectral data cubes from pinto beans that have been mixed with foreign matter. Bands and band ratios have been identified as effective features to develop a classification scheme for detection of foreign materials in pinto beans. A support vector machine has been implemented with a quadratic kernel to separate pinto beans and background (Class 1) from all other materials (Class 2) in each scene. After creating a binary classification map for the scene, further analysis of these binary images allows separation of false positives from true positives for proper removal action during packaging.

Keywords: hyperspectral imaging, image processing, spectral data processing, band ratio, classification, SVM, pinto beans

1. INTRODUCTION

When beans arrive at the conveyor belt for packaging, they may contain unwanted material, such as debris. Before packaging the beans these materials must be detected and removed for high-quality product delivery to the consumer. Unwanted matter can be detected using hyperspectral imaging.

In classical machine vision systems, visual assessment methods are utilized that depend on bean size, color, shape and texture using two-dimensional image processing for object detection or differentiation. In the case of hyperspectral images, myriad image frames at different bands are available in addition to spectral signatures that could be correlated to different objects. Both spectral and spatial information can be analyzed for feature extraction and classification.

Machine vision applications start with the use of an imaging technology to acquire data, followed by data processing for information extraction. In this case a portable hyperspectral imaging system in the visible to near infrared (SOC710, Surface Optics Corp., San Diego, CA, USA) has been used to acquire and view hyperspectral data cubes from pure bean samples and pinto beans artificially contaminated with debris and other foreign material. MATLAB software tool (Mathworks, Inc.) was utilized for hyperspectral data processing and analysis. A support vector machine (SVM) with a quadratic kernel was implemented for the classification of hyperspectral image pixels based on eight bands and band ratios used as effective features. For the two-class SVM-based classification, pinto beans and background were defined as Class 1, and all foreign material as Class 2. In this case, the background was comprised of the gray calibration panel on which the beans and foreign materials were placed. In a factory setting, the background will be the conveyor belt, and the classifier will need to be retrained for the new background.

Background

Hyperspectral imaging has been used for food quality and safety during food processing[1]. Mahajan *et al.* reviewed different machine vision techniques for non-destructive evaluation of legume quality. The authors report that hyperspectral imaging is still an underutilized technology for legume quality analysis compared to other imaging technologies[2]. Walter *et al.* discuss spectral assessment of plant shoots and canopies for phenotype analysis of beans[3]. The authors summarize some of the features used as indicators for plant leaf color, such as normalized difference

*ruby.mehrubeoglu@tamucc.edu; phone 1 361 825-3378; fax 1 361 825-3056

Imaging Spectrometry XX, edited by Thomas S. Pagano, John F. Silny, Proc. of SPIE Vol. 9611, 96110A © 2015 SPIE · CCC code: 0277-786X/15/$18 · doi: 10.1117/12.2207797

vegetation index (NDVI) which is calculated as difference over sum of two different wavebands in the spectral data, one in the visible and one in near-
infrared (NIR) range. Monteiro *et al.* use various vegetation indices (VI) in hyperspectral images to assess biophysical parameters such as leaf area index to predict crop yield[4]. Similar to Water's group, NDVI was used in red and NIR bands to capture energy absorption in the red region by leaves, and reflectance and transmission of energy scattering by individual leaves in the NIR bands.

Gazala *et al.* investigate remote sensing field canopy hyperspectral data to examine spectral reflectance of soybean leaves. The authors' target was to identify effective bands for the detection of Mungbean yellow mosaic India virus on the leaves[5]. The authors identified 445, 589, 642, 686, and 750 nm as effective wavebands for detecting infections due to this virus depending on the color of the leaf, and used both bands and band ratios in their study. Vellaichamy *et al.* experimented with X-ray and NIR hyperspectral imaging to identify diseases in soybean seeds[6]. The authors incorporate linear and quadratic discriminant analysis techniques and combine the two technologies to improve their classification results based on principal component analysis to identify features from X-ray and NIR hyperspectral data. The authors report improved classification results with the combined systems.

Feature identification and extraction is a challenging problem in multivariate data. Rajah *et al.* investigated partial least-squares discriminant analysis (PLS-DA) and variable (in this case waveband) weights in the projection (VIP) scores to identify bands for optimal discrimination of common dry bean varieties during temporal growth studies[7]. The authors show PLS-DA accurately differentiated common bean varieties from field-hyperspectral imaging of the canopy in intermediate to late growth stages. Zhang *et al.* applied chemometrics to hyperspectral images of black beans to differentiate varieties using the wavelength range from 440 to 943 nm[8]. The authors compared PLS-DA, soft independent modeling of class analogy (SIMCA), K-nearest neighbor (KNN), SVM, and extreme learning machine (ELM) classification algorithms and found the ELM algorithm to offer the highest accuracy in classifying the black bean varieties based on the spectral data.

Noordam and van den Broek summarize multispectral imaging in postharvest agricultural products from literature including analysis of potatoes, peppers, and wood. The authors developed a cluster size-insensitive Fuzzy C-Means (csiFCM) algorithm to overcome clusters with small numbers for unsupervised classification of potato skin in terms of healthy, green, and dark spots[9]. For classification, Gualtieri and Chettri used support vector machines to classify soybeans in remote sensing-based hyperspectral data[10]. Compared to the minimum-distance algorithm, the authors report at least 2% improved classification performance with the SVM.

To demonstrate the differentiability of beans from foreign materials, a hyperspectral imaging system has been used to acquire hyperspectral data cubes. In this study, specific wavebands and waveband ratios were investigated as selected features for segmentation of the hyperspectral images and classification of each pixel representing the scene under a supervised learning scheme with the SVM algorithm, as further explained in the Methods section.

2. METHODS

Hyperspectral Data Acquisition

Hyperspectral images were acquired from grocery-bought pinto beans, foreign materials, and images with mixed foreign materials and beans. Foreign materials were artificially added to the scene and included leaves, snail shell, rodent, twigs, bark, rock, pine cone, as well as other items. Images were obtained from only pinto beans, and mixed scenes with foreign matter and pinto beans. Data were collected with SOC710 visible-to-NIR-range (VNIR) portable hyperspectral imaging system (Surface Optics Corp., San Diego, CA) with 696 lines, 520 samples, and 128 bands. The camera has a spectral range of 375 to 1049 nm however only the wavelengths between 400 and 1000 nm were used. The beans and materials were placed on a reference panel which were then imaged together and separately using the system. The reference panel was later used for image normalization purposes.

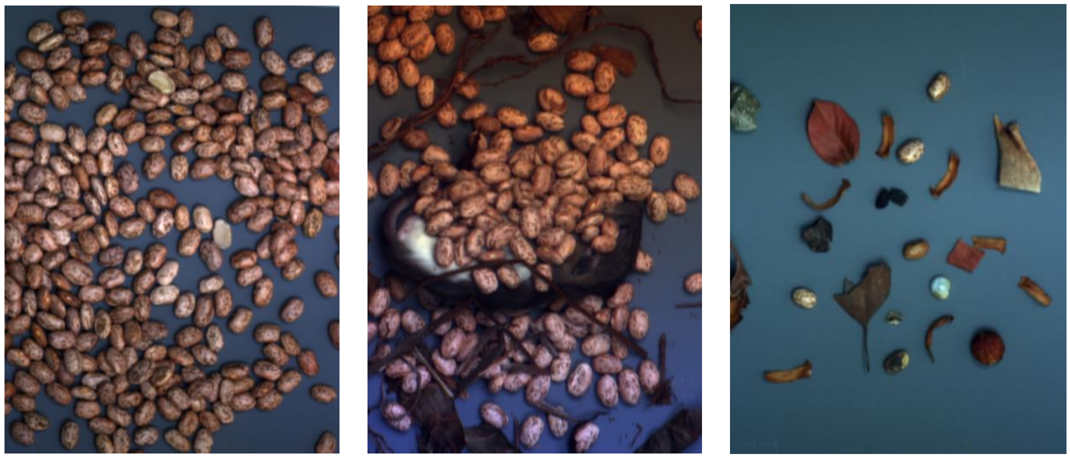

Figure 1. Color representation of (a) pinto beans and (b)/(c) beans with foreign material from hyperspectral data cubes.

Hyperspectral Data Processing

Hyperspectral images were first normalized using the calibration panel image to remove illumination variations within the images. The SOC710 camera automatically removes dark current from each hyperspectral data cube and performs calibration for radiance internally. In this application, after data are acquired, hyperspectral images are normalized by dividing the hyperspectral image pixels representing the scene as spectral signatures, by the reference panel hyperspectral image as in Equation (1):

$$I_N(i,j,k) = I(i,j,k) \,/\, (I_R(i,j,k), \text{ for } i=1,2,3,\dots,M,\ \ j=1,2,3,...,N,\ \ k=1,2,3,\dots,Z, \tag{1}$$

where i is the line number, j is the sample number, and k is the band number, with M = 696, N = 520, and Z = 128. $I(i,j,k)$ is the raw hyperspectral data value at voxel location (i,j,k), $I_R(i,j,k)$ is the reference panel data value at the same location, and $I_N(i,j,k)$ is the resultant normalized data value.

Each pixel in an image frame was assumed to represent an endmember or be a pure pixel. After normalization, the images were smoothed in the spectral dimension using a 5x1 run-length averaging window using Equation (2).

$$I_{NS}(i,j,k) = \frac{1}{5}\sum_{k-2}^{k+2} I_N(i,j,k),\ \forall\ i \in [1,695],\ j \in [1,520],\ k \in [3,126], \tag{2}$$

where $I_{NS}(i,j,k)$ is the normalized then spectrally smoothed hyperspectral image value at the given voxel.

Boundary conditions for the spectral averaging filter were set to be equal to the values from the original spectra for the first two and last two bands in each spectrum being spatially averaged, but were not used in the final data analysis.

The averaging filter in the spectral dimension increases the signal-to-noise ratio for the shaded areas around the borders of the beans which are problematic due to the lighting used.

Hyperspectral Data Features

To identify effective bands, a search algorithm was developed to compute sum of column-wise variances in each image frame represented by each of the wavebands. It is expected that when there is high contrast among objects in the image frame, the variance in the spatial dimension will be high, whereas for low-contrast image frames, the variance will be low. High contrast suggests differentiability among objects.

For each image frame represented by a wave band, column (sample) variances, $v(j,k)$, then sum of column variances, $v_s(k)$, were calculated using Equations (3) and (4):

$$v(j,k) = \frac{1}{M-1}\left(\sum_{i=1}^{M}(I_{NS}(i,j,k) - \bar{I}_{NS}(j,k)\right)^2 \tag{3}$$

$$v_s(k) = \sum_{j=1}^{N} v(j,k), \tag{4}$$

where $\bar{I}_{NS}(j,k)$ is the mean value of each column, j, over the entire lines (696 in this case).

Effective bands were selected by sorting the sum of column variances in the image frames in descending order, and investigating the highest values. The top seven bands with maximum distance among the neighboring frame (band) number was selected. These bands were then used individually or as band ratios to represent features. Visual assessment of bands from normalized spectra was also conducted to check if the selected bands were meaningful as effective features for image segmentation purposes.

A user interface was developed for a supervised learning scheme to allow the user to click on the image frame pixels and identify beans and background (Class 1) and foreign material (Class 2) for a binary segmentation problem. This approach allows user input for the definition of spectra in Class 1 (desired) and Class 2 (undesired) and can be adapted to other legumes besides pinto beans. In this case, the seven selected bands (32, 61, 85, 52, 68, 93, 109) corresponded to wavebands centered at (534, 685, 813, 638, 722, 856, 944) nm. The first five bands were used directly as features. Three band ratios (band ratios 32:61, 52:68, 93:109) were added for a total of 8 features representing each voxel, which were then used for classification using the quadratic kernel-based support vector machines (SVM) algorithm. The number of features was determined manually based on classification success.

For image size of 696x520x128, the band ratios were calculated for every pixel (i,j) representing a line and sample for a total of 696x520 times. The feature vector for each pixel is then defined as

$$\mathbf{f}(i,j) = [I_{NS}(i,j,k_1), I_{NS}(i,j,k_2), I_{NS}(i,j,k_3), I_{NS}(i,j,k_4), I_{NS}(i,j,k_5), I_{NS}(i,j,k_1) / I_{NS}(i,j,k_2), I_{NS}(i,j,k_4) / I_{NS}(i,j,k_5), I_{NS}(i,j,k_6) / I_{NS}(i,j,k_7)], \tag{5}$$

$\forall\ i \in [1, 696]$, $j \in [1, 520]$ and $k_1 = 32$, $k_2 = 61$, $k_3 = 85$, $k_4 = 52$, $k_5 = 68$, $k_6 = 93$, $k_7 = 109$.

$\mathbf{I}_{NS}$ is the normalized image which has been spatially averaged and mean-centered along the spectral direction. $I_{NS}(i,j,k_n)$ is the value in the $\mathbf{I}_{NS}$ image matrix at line i, sample j, and band k_n where $n \in [1,2,3,\ldots,7]$.

Classification

SVM algorithm was used for classification. For the supervised training data set, background and bean pixels were grouped into Class 1, and unwanted matter was grouped into Class 2. Because of the significant differences in spectral characteristics in the normalized bean and background pixels in Class 1, training was achieved using a quadratic kernel. Testing was performed on the same image as well as independent images of beans and mixed materials shown in Figure 1 (a) through (c). MATLAB software tool was used for the application of the SVM algorithm to the hyperspectral data. Then a binary image was created based on the results of the classifier showing regions belonging to Class 1 in black, and Class 2 in white. This binary classification map was used as a template, and then median filtered by a 3x3 filtering window to reduce salt and pepper noise. Then the template was multiplied with the original image frames of choice, or RGB image to demonstrate areas of identified foreign materials. The segmented binary image identifying regions of interest representing foreign matter was further analyzed to discard any false positives in the binary classification map.

3. RESULTS AND DISCUSSION

Figure 2 shows different levels of contrast in hyperspectral images based on the image frame and waveband.

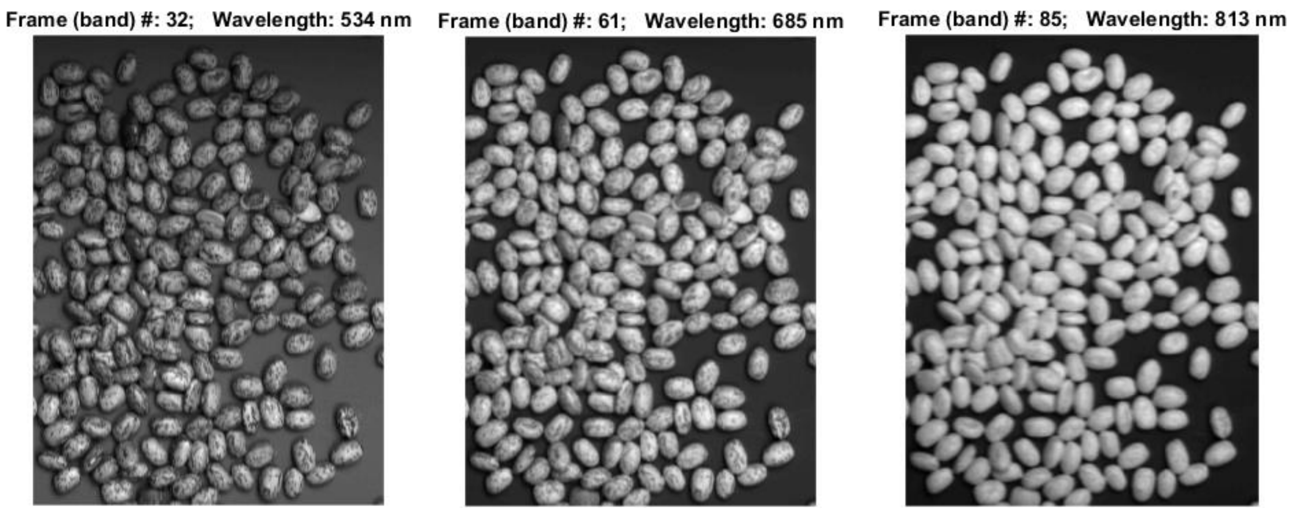

(a) **(b)** **(c)**

Figure 2. Pinto beans on reference panel. Pinto beans at waveband (a) 32 (534 nm) (b) 61 (685 nm) (c) 85 (813 nm)

It is clear from Figure 2 that at band 85, the spotted/freckled nature of the pinto beans seems to reduce. The contrast between pinto bean spots and pinto bean body reduces as the waveband number is increased. Bean spots and bean body are not visibly differentiable at higher wavelengths although beans and certain foreign materials are, deeming features based on higher wavelengths effective.

The SVM classifier was trained using the hyperspectral image cube represented by the mixed materials color image in Figure 1 (c) following the procedure detailed in the Methods (Section 2). The user identified pixels representing beans and background from this image as well as debris.

Average normalized spectra for different materials are represented in the Figure 3 below:

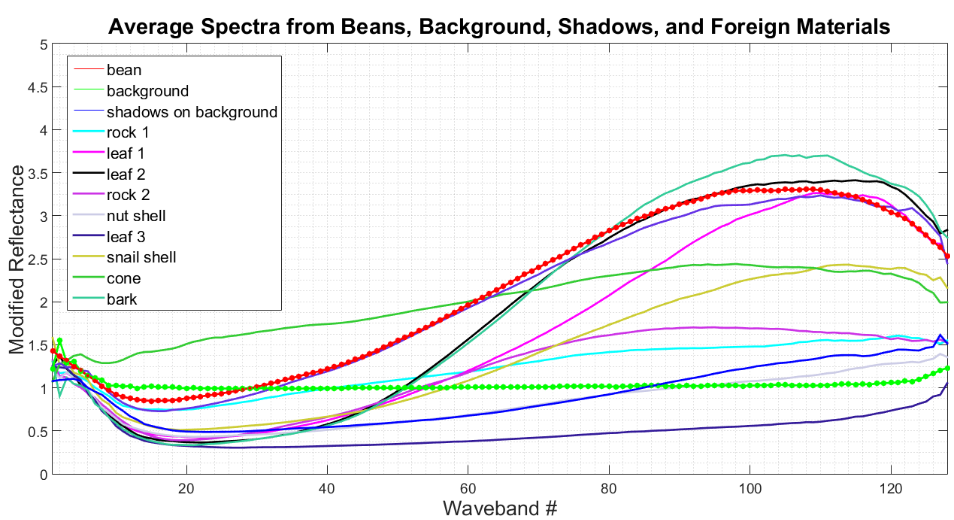

Figure 3. Average spectral representation of different materials (horizontal axis: wavebands (1-128) corresponding to wavelengths 376-1049 nm; vertical axis: modified reflectance). Dotted lines represent spectra from Class 1 (beans and background).

Figure 4 through Figure 7 show the classification results based on binary segmentation from SVM classifier. The rightmost image in each figure demonstrates the detected foreign material obtained by applying the binary template over the original image.

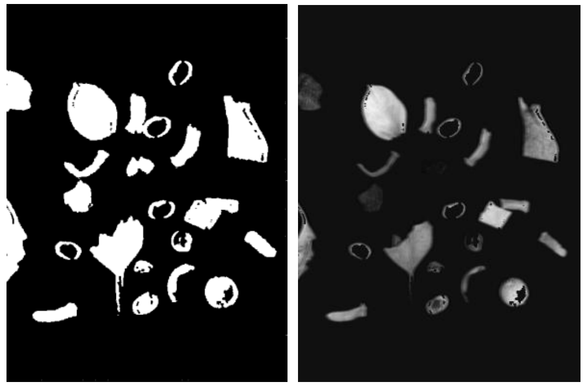

Figure 4. SVM segmentation and classification results for the training image of Figure 1 (c)

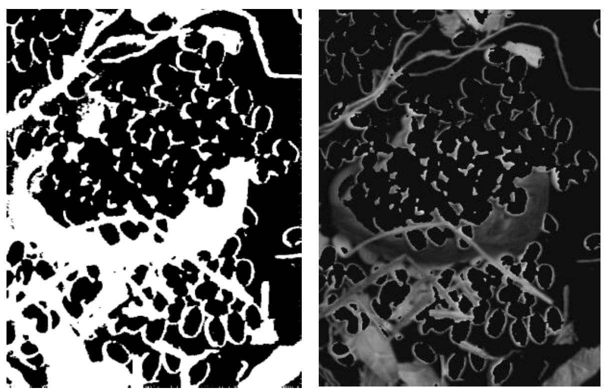

Figure 5. SVM segmentation and classification results for independent image shown in Figure 1 (c)

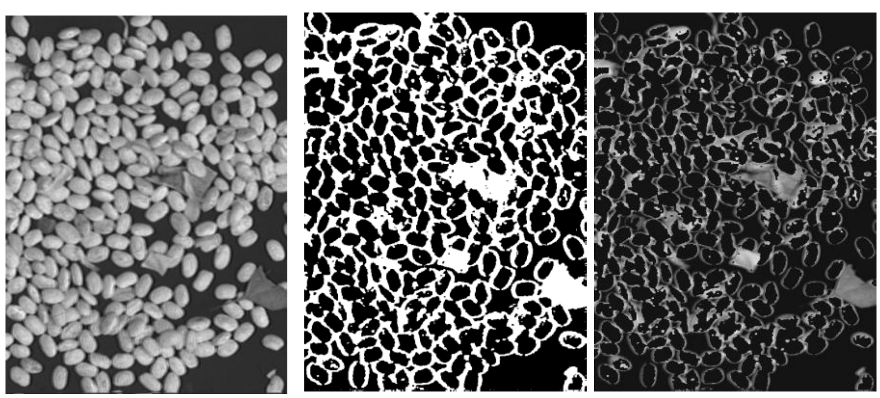

Figure 6. SVM segmentation and classification results for an independent image with beans and debris (leaves, bark, etc)

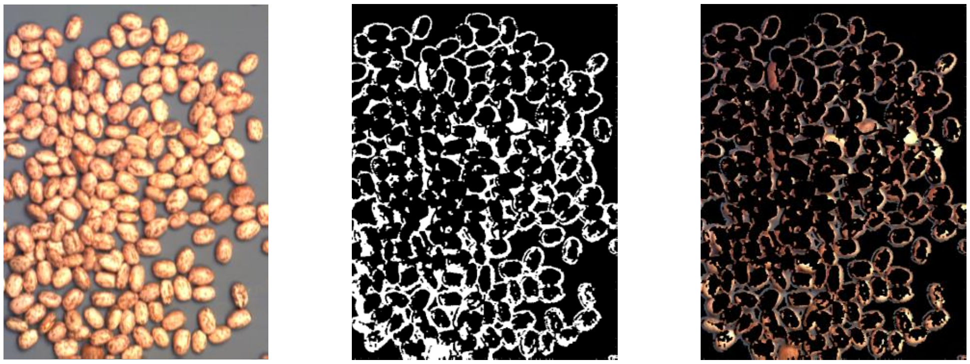

Figure 7. Detection of potentially ‘bad beans’ in a bean-only image

Figure 8. Detection of the rodent in an image with no beans.

The above images show the preliminary results in separating foreign materials from beans. The shadows caused by the bean shape produce erroneous classification of results and must be addressed. One way to address this problem is through template matching applied in the spatial domain to differentiate beans from other materials based on shape. Another method is to investigate the number of high (white) pixels in the binary images, and setting a threshold to eliminate or keep the regions identified as foreign matter. One line-by-line summation-based selection process is demonstrated in Figure 9. Gray areas in the middle image indicate potential locations of foreign material. In this particular case, foreign material is found in almost all rows.

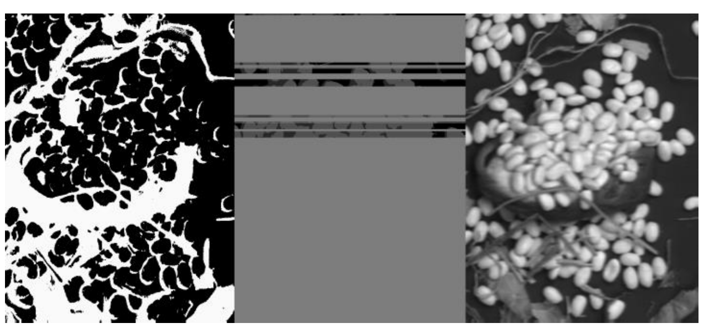

Figure 9. Improved selection of areas that contain foreign material (middle, solid gray). The selection process is based on horizontal line sums in the binary mask image (left) that identifies the potential locations of foreign material in the original image (right). After line sums are obtained, thresholding of the row sum values reveals the areas with foreign material that requires attention (middle, solid gray).

4. SUMMARY AND CONCLUSIONS

Pinto beans and other biological matter have been imaged using a portable hyperspectral imaging system to differentiate unwanted materials from the beans. Spectral signatures from each object have been spectrally smoothed to increase signal-to-noise ratio and then to determine wavebands that effectively separate beans and background from foreign materials. Waveband ratios have also been investigated as features to differentiate foreign matter from pinto beans. The SVM was used for classification to generate binary maps showing the regions with potential foreign material among the beans. Median filtering was applied to the binary map to remove salt and pepper noise. This work demonstrates hyperspectral imaging as a potentially effective method to achieve identification of foreign matter from its spectral signatures and identifies areas of interest through binary image segmentation and mapping of the two classes in the 2D representation of the scene. The issues with shadows on the bean borders could be reduced with alternative lighting solutions, as well as template matching trained on pinto beans in the spatial domain and applied on the final segmented images.

ACKNOWLEDGEMENT

The authors would like to thank Wes Autran for his contributions to the collection of data. This project has been supported by Surface Optics Corp.

REFERENCES

[1] Stier, R. F., "Foreign Material Control: Food Quality, Safety or Both?" Food Safety Magazine (Apr/May 2014). (Available: http://www.foodsafetymagazine.com/magazine-archive1/aprilmay-2014/foreign-material-control-food-quality-safety-or-both/ (last accessed July 3, 2015).

[2] Mahajan, S., Das, A. and Sardana H. K., "Image acquisition techniques for assessment of legume quality," Review, in Trends in Food Science & Technology 42, 116-133 (2015).

[3] Walter, A., Liebisch, F. and Hund, A., "Plant phenotyping: from bean weighing to image analysis," Plant Methods 11-14 (2015).

[4] Monteiro, P. F. C., Filho, R. A., Xavier, A. C. and Monteiro R. O. C., "Assessing biophysical variable parameters of bean crop with hyperspectral measurements," Scientia Agricola, 69(2), 87-94 (2012).

[5] Gazala, I. F. S., Sahoo, R. N., Pandey, R., Mandal, B., Gupta, V. K., Singh, R., and Sinha, P., "Spectral reflectance pattern in soybean for assessing yellow mosaic disease," Indian J. Virol., 24(2), 242-249 (2013).

[6] Vellaichamy, C., Karuppiah, K. and Jayas, D. S., "Detection of *Callosobruchus machulatus* (F.) infestation in soybean using soft X-ray and NIR hyperspectral imaging techniques," J. Stored Products Research, 57, (2014). DOI: 10.1016/j.jspr.2013.12.005

[7] Rajah, P., Odindi, J., Abdel-Rahman, E. M., Mutanga, O., and Modi, A., "Varietal discrimination of common dry bean (*Phaseolus vulgaris* L.) grown under different watering regimes using multitemporal hyperspectral data," Journal of Applied Remote Sensing, 9, 096050-1 – 096050-14 (2015).

[8] Zhang, C., Liu, F., Zhang, H. L., and He, Y., "Identification of varieties of black bean using ground based hyperspectral imaging," Spectroscopy and Spectral Analysis, 34(3), 746-50 (2014).

[9] Noordam, J. C., van den Broek, W. H. A. M, "Clustering and classification of multispectral imaging for quality inspection of postharvest products," in [Techniques and applications of Hyperspectral Image Analysis], H. F. Grahn and P. Geladi, Ed.s, John Wiley & Sons Ltd., Chichester, 43-67 (2010).

[10] Gualtieri, J. A. and Chettri, S., "Support vector machines for classification of hyperspectral data," IEEE Proc. IGARSS Conf., (2000)